

MERLIN observations of Stephan’s Quintet

E. Xanthopoulos^{1,2,3}, T. W. B. Muxlow³, P. Thomasson³, S. T. Garrington³

¹*University of California Davis, Department of Physics, Davis, CA 95616*

²*IGPP/Lawrence Livermore National Laboratory, Livermore, CA 94550*

³*University of Manchester, Jodrell Bank Observatory, Macclesfield, Cheshire SK11 9DL, England*

Accepted . Received

ABSTRACT

We present MERLIN L-band images of the compact galaxy group, Stephan’s Quintet. The Seyfert 2 galaxy, NGC 7319, the brightest member of the compact group, is seen to have a triple radio structure typical of many extra-galactic radio sources which have a flat spectrum core and two steep spectrum lobes with hot spots. The two lobes are asymmetrically distributed on opposite sides of the core along the minor axis of the galaxy. Ultraviolet emission revealed in a high resolution HRC/ACS HST image is strongly aligned with the radio plasma and we interpret the intense star formation in the core and north lobe as an event induced by the collision of the north radio jet with over-dense ambient material. In addition, a re-mapping of archive VLA L-band observations reveals more extended emission along the major axis of the galaxy which is aligned with the optical axis. Images formed from the combined MERLIN and archive VLA data reveal more detailed structure of the two lobes and hot spots.

Key words: galaxies: cluster – galaxies: interactions – individual: Stephan’s Quintet, NGC 7319, NGC 7318A and B.

1 INTRODUCTION

Stephan’s Quintet (also known as Arp319 and VV228), which can be regarded as the prototype of the compact group class of galaxies (H92 in the Hickson 1982 catalog), was the first to be discovered 120 years ago by Stephan (1877). It has been studied intensively in almost every wavelength domain and it is a remarkable example of a group of galaxies visited by infalling neighbours.

There has been much controversy regarding the redshifts of its galaxies and their nature. The members of the group (Fig. 1) were initially thought to be NGC 7317, NGC 7318A, NGC 7318B, NGC 7319, NGC 7320 and NGC 7320C. However, it was later found that NGC 7318B had a velocity almost 1000 km s^{-1} lower than the mean redshift of the group ($\approx 6600 \text{ km s}^{-1}$) and NGC 7320 was at a redshift of only $\approx 800 \text{ km s}^{-1}$. Moles et al. (1997) have argued that the discordant-redshift galaxy, NGC 7320, is an unrelated foreground galaxy and have suggested that the kernel of three galaxies, NGC 7317, NGC 7318A and NGC 7319, has been visited by two “intruders” (NGC 7320C and NGC 7318B) at different times in the past few 10^8 years. As a result of these “intrusions”, the intragroup medium has been filled with HI gas, stripped from the spiral members of the group

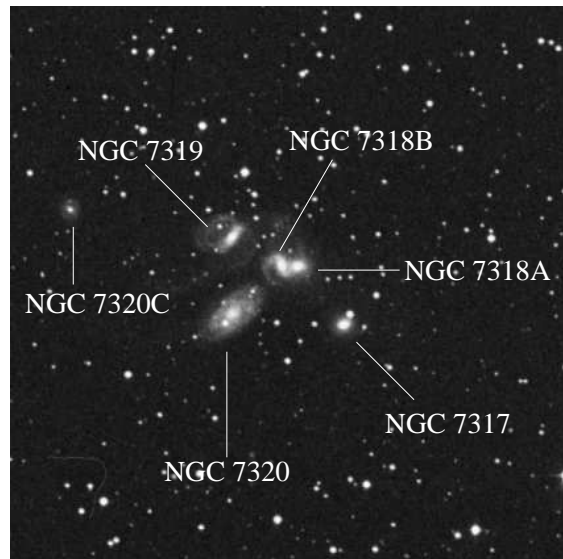


Figure 1. Digital Sky Survey map covering the member galaxies of Stephan’s Quintet.

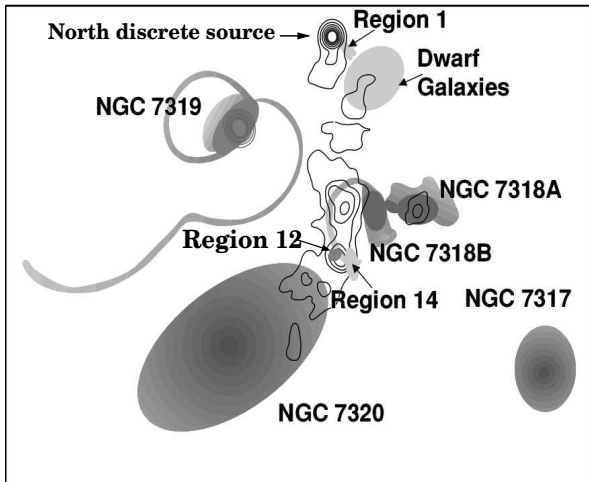


Figure 2. Schematic showing the relative positions of the radio emission detected by van der Hulst & Rots (1981) and the optically visible galaxies. Also shown are the locations of a group of dwarf galaxies and regions of $H\alpha$ emission, designated Regions 1, 12 and 14 by Mendes de Oliveira et al. (2001). Both the dwarf galaxies and $H\alpha$ emission are considered to be associated with NGC 7318B.

(Allen & Sullivan 1980; Sulentic & Arp 1983; Shostak et al. 1984; Pietsch et al. 1997; Williams 1998).

Allen & Hartsuiker (1972) produced the first continuum radio image of Stephan’s Quintet at a wavelength of 21 cm using the Westerbork Synthesis Radio Telescope. At a resolution of $\approx 20'' \times 45''$, it showed an unresolved source coincident with NGC 7319, and an unusual semi-circular arc of emission which appeared to envelop it. Since then, VLA observations at 20 cm wavelength by van der Hulst & Rots (1981) with a resolution of $6''$ have shown more clearly the main components of the radio emission associated with Stephan’s Quintet. These are shown in the schematic in Fig. 2. More recent VLA observations at 3.6 cm, 6 cm and 20 cm by Aoki et al. (1999) show that the source centered on NGC 7319 has three compact components, aligned perpendicular to the disc of the galaxy and embedded in more diffuse emission. According to Aoki et al. (1999), all the components of the emission have steep spectra which, they indicate, is commonly found in Seyfert galaxies. Van der Hulst & Rots (1981) resolved the arc of emission between NGC 7319 and NGC 7318B into distinct sources embedded in more diffuse emission which is partly coincident with spiral-arm-like features in NGC 7318B. They considered this arc of emission to be more like a letter “W” on its side, associating it with the starburst region. They also noted a discrete, unresolved source, just to the north of the “W”, which, with no optical counterpart, they considered to be an unrelated background object.

In this paper, high resolution MERLIN radio observations at L band (18 cm) are presented for the first time. Also presented are the results of a re-analysis of L band (20 cm) VLA archive data and a combination of this and the MERLIN data to reveal in much more detail the structure of the radio emission, not only of NGC 7319, but of the hitherto unresolved sources in the field. An archival near-UV high

resolution HST image of NGC 7319 is also analyzed and the UV, optical and radio emission correlation is examined and discussed. In Section 2, the MERLIN and HST observations and data analysis as well as a re-analysis of the VLA data are described. Maps and results are included in Section 3 and the paper finishes with a discussion and conclusions. Throughout this paper we use $H_0 = 65 \text{ km s}^{-1} \text{ Mpc}^{-1}$ unless otherwise specified. $1''$ corresponds to 485 pc at the redshift $z=0.02251$ of NGC 7319.

2 OBSERVATIONS & DATA REDUCTION

2.1 MERLIN data

Observations of Stephan’s Quintet were made with MERLIN at L band in April and June 1999. A bandwidth of 16 MHz in both left and right circular polarizations was used, centered on 1658.0 MHz. The observations were made in “wide-field” mode in order to cover as much as possible of the environment of Stephan’s Quintet. The total extent of Stephan’s Quintet is $\approx 6 \times 6 \text{ arcmin}^2$ which is easily accessible to MERLIN in its “wide field” mode with a field of view at L band of $\approx 20 \times 20 \text{ arcmin}^2$, though with image-smearing towards the edges of the field. In this mode, the cross-hands of polarization (LR and RL) are not correlated in order to increase by a factor of 2 the number of channels into which the 16 MHz LL and RR correlations can be divided; i.e. 32 channels of 0.5 MHz bandwidth. By preserving these 0.5 MHz bandwidth channels in the subsequent processing, it is this 0.5 MHz and not the full 16 MHz bandwidth correlated that determines the field of view. Thus the angular radius from the pointing centre at which a 10% image smearing due to the 0.5 MHz ‘bandwidth’ occurs is ≈ 4.7 arcminutes. The integration time per data point was 4 seconds, which would give rise to a 10% integration time smearing at an angular distance from the pointing centre of ≈ 5.3 arcminutes. The pointing centre for the MERLIN observations was at $\alpha = 22^{\text{h}}36^{\text{m}}00.51^{\text{s}}$ and $\delta = 33^{\circ}58'03''.76$ (J2000). Observations of Stephan’s Quintet were interleaved with those of a nearby phase calibration source, 2243+357, with a total cycle time (including telescope drive times) of 7.5 min (5.5 min on source, 2 min on the calibrator). Although the total on source time was ≈ 70 hours, one or more telescopes were lost for significant periods of time during the observations because of weather conditions; i.e. wind.

The data were edited, corrected for elevation-dependent effects, non-closing baseline errors and bandpass response using the standard MERLIN analysis programs. The flux calibration was established from observations of 3C286, whose flux was computed to be 13.639 Jy at 1658 MHz on both the scale of Baars et al. (1977) and the VLA calibration list. The telescope relative sensitivities, bandpass and non-closing corrections were obtained from observations of the point source OQ208, whose flux density was determined to be 1.18 Jy from a comparison of its signal amplitude with that from 3C286 on the shortest MERLIN baseline.

After combining the data from the different days, further processing was carried out using the MERLIN automated pipeline procedure, which uses the NRAO AIPS tasks. In this, the target source (Stephan’s Quintet) was mapped after its data had been corrected for further amplitude and

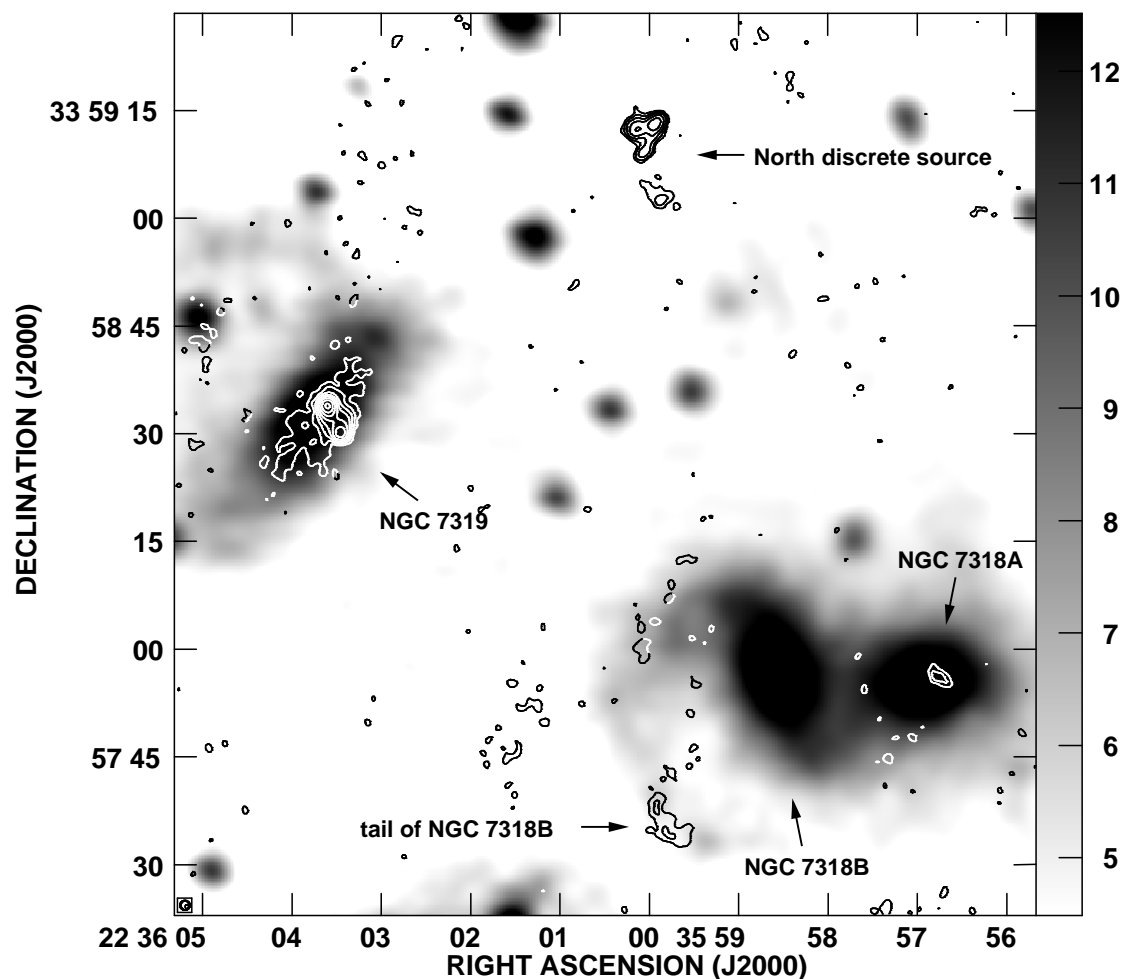


Figure 3. 20 cm naturally weighted VLA archive data image of Stephan's Quintet at a resolution of $1''.3$ overlaid on a Digital Sky Survey image. Contour levels are at $6.97e-5 \times (1, 2, 4, 8, 16, 32, 64, 128, 256)$ Jy/beam. The peak flux is 10.3 mJy/beam and the rms noise level is $\sim 27 \mu\text{Jy}/\text{beam}$.

phase errors derived as a result of mapping the phase-calibration source, 2243+357. Finally, those fields within the MERLIN primary beam showing radio emission were carefully mapped using different data weighting functions to produce the final images.

2.2 VLA data

Although the observations of Aoki et al. (1999) were directed solely at the Seyfert galaxy, NGC 7319, within Stephan's Quintet, it has been possible to use the data from their 20 cm observations on 4 November 1996 (VLA programme AA206) to produce a 20 cm image of a much wider field. The data were obtained from the VLA archive, together with corresponding observations of the flux and baseline calibrator, 3C48, and a phase reference source, 2236+286. The flux density of 3C48 in the two IFs centered at 1364.9 MHz and 1435.1 MHz were taken to be 15.617 Jy and 16.319 Jy respectively, based on the VLA calibration scale. As for the

MERLIN observations, after initial calibration using 3C48, the data were corrected for additional amplitude and phase errors derived as a result of mapping the phase calibration source. The images obtained solely from the VLA data, were produced using the NRAO AIPS tasks.

Finally, after ensuring correct positional and flux scale alignment, images of those fields showing radio emission within the primary beam of the telescope were produced from the combined MERLIN+VLA data. The maps for the northern discrete source and for NGC 7319 are shown in Fig. 4 and Fig. 6 respectively. The resolution of the combined data is $0''.15$ and the rms noise level is $30 \mu\text{Jy}/\text{beam}$. Although the core emission (component B) of NGC 7319 is now less obvious than in the MERLIN only image as it blends into the extended emission, the overall structure of NGC 7319 and, in particular, the structure of the previously unidentified northern source are now much more clear.

2.3 HST/ACS data

An HST image of NGC 7319 was obtained in 2002 with the High Resolution Channel (HRC) of the ACS camera as part of the HST proposal 9379 on Near Ultraviolet imaging of Seyfert galaxies. The image was taken through the F330W (HRC U) filter (effective wavelength 3354Å/ 588Å) with a 1200 sec exposure. The HRC has a $29'' \times 25''$ field of view and a plate scale of $\sim 0.027''$ pixel. Basic two-dimensional image reductions (overscan, bias, dark subtraction and flat fielding) as well as cosmic ray rejections from the CR-SPLIT=2 data were performed with the CALACS pipeline processing. The observations used the dither patterns and so further processing by PyDrizzle corrected for geometric distortion of the ACS camera and combined the dithered images into one final reduced and calibrated image. Using IRAF we removed any remaining cosmic ray events from the data and rotated the image to the cardinal orientation (North up and East to the left) by means of the keyword "ORIENTAT" in the data header. At the redshift $z=0.0225$ of the galaxy, 1 pixel corresponds to 13.1 pc for $H_0 = 65 \text{ km s}^{-1} \text{ Mpc}^{-1}$.

The final calibrated reduced ACS image is shown in Fig. 7. The Ultraviolet observation through the F330W filter is the optimal configuration to detect faint star forming regions around the nuclei. The image, calibrated in counts in e^- , was multiplied by the PHOTFLAM keyword from the image header and converted to $\text{erg cm}^{-2} \text{Å}^{-1}$. A U magnitude of 16.01 was measured using the zero point, PHOTZPT.

3 MAPS AND RESULTS

3.1 Stephan Quintet's radio detections

The resulting naturally weighted VLA map of Stephan's Quintet with a beam size of $1''.3$ is shown in Fig. 3 (rms noise level $27 \mu\text{Jy}/\text{beam}$). The total intensity contour map is overlaid of the optical Digital Sky Survey image of the same area. The lowest believable contour is at a level of approximately a factor of 2 lower than that in the published map of NGC 7319. The improvement in this image is probably due in part to taking into account all of the radio emission in the field in the 'reconstruction' of the image from the data. As might be expected, in comparison with the MERLIN images, this shows the extended structure more clearly, though even at this resolution, much of the north-south arc of emission is considerably resolved and the emission that is visible in the region at $\alpha \approx 22^{\text{h}}35^{\text{m}}59.8^{\text{s}}$, $\delta \approx 33^{\circ}57'34''$ (J2000) is at the limit of sensitivity. However, the northern unidentified source is clearly visible, though somewhat resolved. Also visible in the image is radio emission at a position corresponding to the core of NGC 7318A. More specifically the radio detections in the VLA image are:

a) NGC 7318A: The two elliptical contours seen at $\alpha = 22^{\text{h}}35^{\text{m}}56.8^{\text{s}}$, $\delta = 33^{\circ}57'55''$ (J2000) (Fig. 3), correspond to the centre of NGC 7318A. This is the weak radio detection also mentioned by van der Hulst & Rots (1981), Menon (1995), Williams et al. (2002) and Xu et al. (2003) who measured 1.3, 0.8, 1.4 and 0.95 mJy, respectively. Our measured flux density is slightly lower, $\approx 0.61 \pm 0.01$ mJy. Bushouse (1987) reported detection of modest H α emission from the

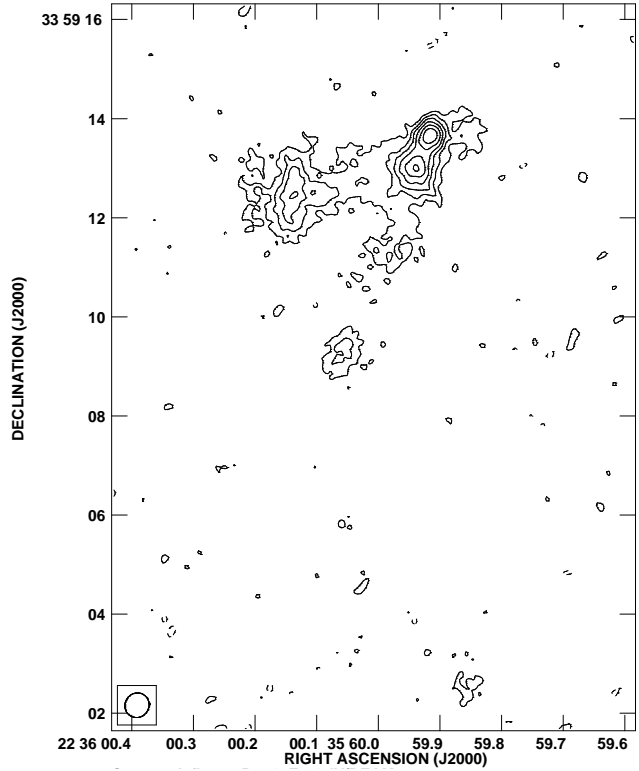


Figure 4. VLA+MERLIN combined L band map (resolution $0''.15$) of the north discrete source. The contour levels have been set to $7.59\text{e-}5(-1,1,2,3,4,5,6,7,8,9,10)$ Jy/beam. The peak flux is $527 \mu\text{Jy}/\text{beam}$ and the rms noise level is $\sim 30 \mu\text{Jy}/\text{beam}$.

nuclear region of NGC 7318A although more recently Moles et al. (1998) did not detect any emission from NGC 7318A using longslit spectroscopy. NGC 7318A is completely resolved by our MERLIN only observations.

b) Tails of NGC 7318B: The radio emission at the map sensitivity limit seen at the southerly position $\alpha = 22^{\text{h}}35^{\text{m}}59.8^{\text{s}}$, $\delta = 33^{\circ}57'34''$ (J2000) in Fig. 3 is all that remains at this resolution of the arc of emission, probably related to the southern tail of NGC 7318B and in particular to the bright emission-line regions 12 and 14 as labelled by Mendes de Oliveira et al. (2001). These regions are examples of non-rotating structures, possibly associated with HII regions and have star formation rates of $\sim 0.1 M_{\odot} \text{ yr}^{-1}$. They are regions rich in cold and ionized gas.

c) The North Discrete Source: The unidentified source seen at the northern end of the arc of radio emission between NGC 7319 and NGC 7318B was first mentioned by van der Hulst & Rots (1981), who could not, however, unambiguously say whether this source was associated with Stephan's Quintet or whether it was an unrelated background source. The MERLIN+VLA image of it is shown in (Fig. 4). The image indicates that the source is still something of an enigma. Xu et al. (2003) identify the binary radio source in VLA 1.4 and 4.86 GHz images as the cosmologically distant background source seen in projection behind SQ (van der Hulst & Rots 1981, Williams et al. 2002), and note that there is no

optical counterpart brighter than 29 mag arcsec⁻² (Williams et al. 2002), nor any IR counterpart in the ISO images (Xu et al. 1999, Sulentic et al. 2001). The total measured flux density from our radio images, including the southernmost component at $\alpha = 22^{\text{h}}35^{\text{m}}59.85^{\text{s}}$, $\delta = 33^{\circ}59'02''$ (J2000), is 7.16 ± 0.5 mJy. This flux is less than the 9 mJy flux measured by van der Hulst & Rots (1981), and 10.3 mJy measured by Xu et al. (2003) and Williams et al. (2002), indicating that more extended weak emission has been resolved.

Although it has been assumed that this is a background source, it seems a remarkable coincidence that it almost appears to be a continuation of the extended arc of emission thought to be associated with NGC 7318B and therefore with Stephan's Quintet. In the NVSS image of the region with an angular resolution of $45''$, it can be seen that there is extended emission to the northwest of NGC 7319 which extends beyond and to the south-west of the unidentified source position. The peak of this extended continuum emission does not coincide with the unidentified source, but does encompass the dwarf galaxies and emission line regions (1A and 1B) associated with NGC 7318B as found by Mendes de Oliveira et al. (2001) (indicated as Dwarf Galaxies and Region 1 in Fig. 2). The peak of the radio emission seen in the MERLIN+VLA image lies just to the north-east of Region 1. The positional offset is similar to that of the radio emission (still visible in our new VLA image at the southern end of the arc) from the bright emission line region 14 found by Mendes de Oliveira et al. (2001).

3.2 NGC7319

3.2.1 Radio

Aoki et al. (1999) have indicated that the previously known compact components (labelled A, B and C in Fig. 5 after Aoki et al. 1999) and diffuse emission of NGC 7319 all have steep spectra. However, our MERLIN only 20 cm image (Fig. 5), which resolves out much of the extended emission, indicates component B to be unresolved and to have a flux 1.07 mJy, which is very comparable with the value of 1 mJy quoted by Aoki et al. (1999) for its 6 cm flux. At the same time the flux densities of components A and C shown in Table 1, although lower than the 20 cm VLA fluxes measured by Aoki et al. (1999), are more than double in flux than the 6 cm flux densities quoted by Aoki et al. (1999) (see their Table 1). Component B then would appear to have a flat spectrum, and as such is considered to be the core of the galaxy. We are also able to measure a size for component B. This could not be defined by Aoki et al. (1999) due to the closeness of components A and B, and indeed a merging of these components in their 20 cm map. The positions, flux densities, and sizes (FWHM) of the three compact components were measured using the AIPS task JMFIT, a two-dimensional elliptical Gaussian fitting program. These parameters are given in Table 1. The sizes are given after deconvolution from the beams.

The radio structure of NGC7319 looks like a small, asymmetric FR II radio source, with a flat-spectrum core and two extended lobes, both containing compact hot-spots. There is no evidence of a jet as is often the case. However, the size, luminosity and spiral host galaxy of NGC 7319 is consistent with it being a Seyfert 2 galaxy (Durret 1987).

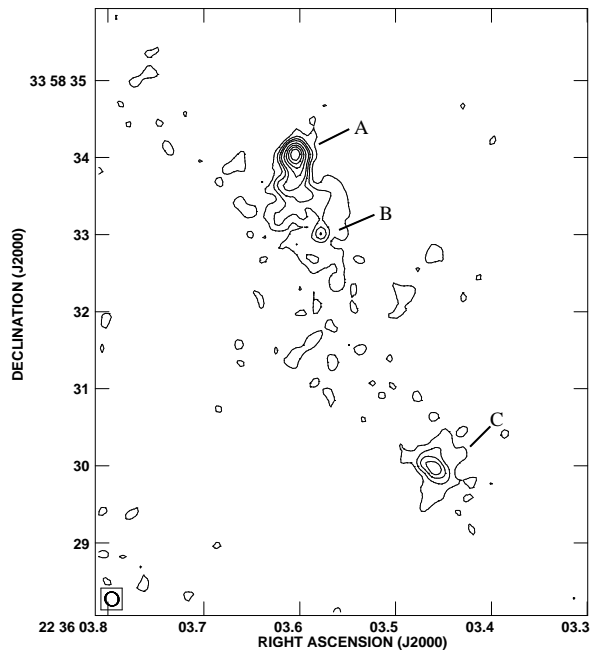


Figure 5. 20 cm naturally weighted MERLIN image of NGC 7319 (resolution $0''.15$). The compact components are labelled A, B and C. Contour levels are set to $1.22e-4 \times (-1, 1, 2, 4, 8, 16, 32)$ Jy/beam. The peak flux is 1.84 mJy/beam and the rms noise level is ~ 47 μ Jy/beam.

The asymmetric arm ratio of 1:3.1 for the distances between the core (component B) and the two hotspots (components A and C respectively) possibly indicates that material to the north-east is blocking the outflow of plasma in that direction whereas plasma outflow to the south-west is much less inhibited.

High resolution radio surveys of Seyfert galaxies (eg. Thean et al. 2000; Thean et al. 2001 and references therein) show that Seyfert 1 and 2 galaxies have a range of radio structures and sizes. At $0''.25$ resolution, the majority are unresolved or only marginally resolved, but approximately 10% show double structures and a similar fraction show triple or multi-component linear structures.

NGC 7319 has a radio luminosity typical of a Seyfert 2 galaxy and a linear size at the upper end of the size distribution. It's FR II-like (such as Cygnus A - which have very well collimated jets ending at high surface brightness hotspots and large diffuse lobes) structure is similar to NGC 5929 (Su et al. 1996), Mrk 463 (Kukula et al. 1999) or IC 5063 (Morganti et al. 1998). The identification of a growing number of Seyferts with a simple FR II-like triple structure is providing increasing evidence for the presence of shocks due to the interaction of radio jets with the ISM in the inner few kpc and calling into question the usual assumption that the compact radio components of Seyfert galaxies, which often closely correspond to peaks in the NLR emission, represent the galaxy nucleus. If NGC 7319 were at twice the distance, components B and C would probably not be detected and

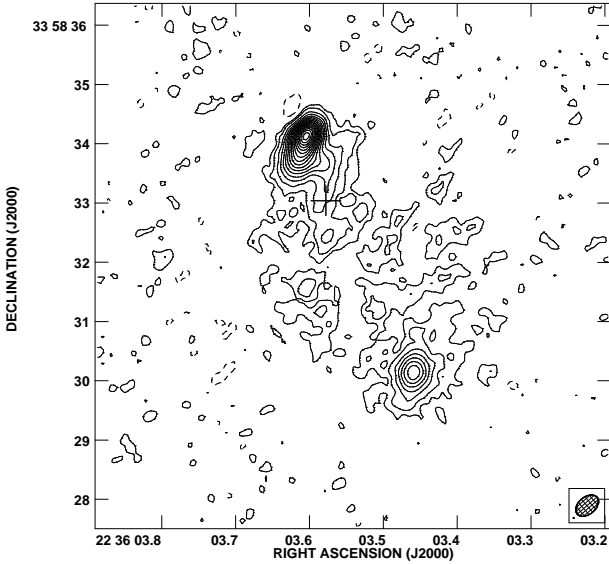


Figure 6. VLA+MERLIN combined L band map of NGC 7319 (resolution $0''.15$). The contour levels have been set to $7.59e-5 \times (-1, 1, 2, 4, 6, 8, 10, 12, 14, 16, 18, 20, 22, 24, 26, 28, 30, 32, 34, 36, 38, 40)$. The peak flux is 3.25 mJy/beam and the rms noise level is ~ 29 μ Jy/beam. The cross indicates the position of the B component (core) as labelled in Fig. 5.

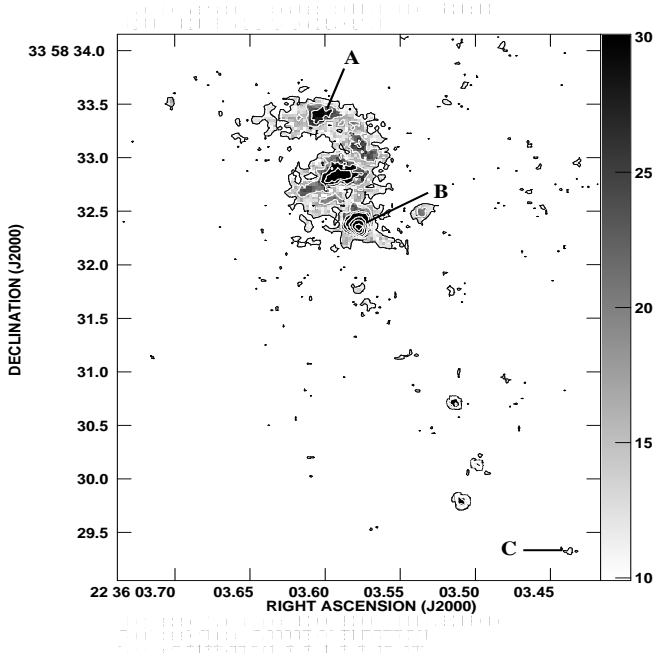


Figure 7. HST ACS/HRC UV (F330W) image of NGC 7319 (resolution $0''.027$). Components A, B and C are indicated in the image. North is up and East to the left. The sidebar shows the relative intensity of the greyscale image. Contour levels are overlaid to accentuate features and are set at $2.0e-20 \times (1, 2, 4, 6, 8, 10, 12)$ erg $cm^{-2} \text{\AA}^{-1}$.

it would be assumed that A is a barely resolved single component Seyfert galaxy.

In addition to the known three compact components and diffuse emission aligned along the minor axis of NGC 7319, the new image formed from the VLA archive data also shows, for the first time, emission of extent $\approx 20''$ perfectly aligned with the strong bar at a PA = 142° (Durret 1987), which is also the position angle of the major axis of the ‘optical’ Seyfert galaxy. Assuming a heliocentric systemic velocity of 6740 km s^{-1} , this corresponds to ~ 9.7 kpc for $H_0 = 65$ km s^{-1} Mpc $^{-1}$. Being close to the limit of detection, only an approximate estimate for its flux can be made and this value is 5.6 ± 0.3 mJy. This weak extended emission, may be associated with backflow from the lobes of the ‘double’ radio source. However, it may also be associated with star formation in the nuclear region of this interacting galaxy and be unrelated to the radio lobes. Assuming the latter to be true, and using the formulae given in Mobasher et al. (1999), $SFR_{1.4} = \frac{L_{1.4}}{8.07 \times 10^{20} WHz^{-1}} M_\odot \text{ yr}^{-1}$, it is possible to calculate a star formation rate for the Seyfert galaxy of $8.4 M_\odot \text{ yr}^{-1}$, from the monochromatic luminosity at 1.4 GHz $L_{1.4} = 6.89 \times 10^{21} WHz^{-1}$ (once again assuming a value for H_0 of 65 km s^{-1} Mpc $^{-1}$ and $z=0.02251$ for NGC 7319). A 10.2 ± 0.5 mJy flux density was also measured from the VLA data for the extended emission along the minor axis.

The total MERLIN flux of NGC 7319 is 12.61 ± 0.5 mJy. This value is much lower than $\sim 28.5 \pm 0.5$ mJy measured by Van der Hulst & Rots (1981), Aoki et al. (1999), Williams et al. (2002) and Xu et al. (2003). This is expected as in the high resolution MERLIN image, most of the extended diffuse emission has been completely washed out. This diffuse emission however is pronounced in the VLA+MERLIN map (Fig. 6) extending between components A and C. The core, component B, is now lost in the diffuse emission and we mark its position, as defined from the MERLIN only map, with a cross in Fig. 6.

3.2.2 Comparing radio and ultraviolet images

It is unfortunate that although the angular resolution of the MERLIN and HST images is $0''.15$ and $0''.027$ respectively, due to absolute astrometric uncertainties for HST data, registration of the two images can not be better than $0''.5$. This problem can be mitigated in cases where there is a bright compact core in the HST image which is reasonably assumed to be associated with the compact inverted spectrum radio core. Aoki et al. (1999) attempted to align HST/WFPC2 and VLA data for NGC 7319 using more accurate astrometric coordinates for the HST image by smoothing the HST image to ground-based seeing and assigning an absolute position for the nucleus determined by ground-based astrometry (Clements 1983). However, the registration caused a systematic separation of $\sim 0''.7$ between features in HST and radio images which is larger than the uncertainties in the Clements’ position. Due to this and also to more systematic differences between the optical and radio astrometric frames they resorted to shift the optical peak onto the position of the radio component B with a resulting shift in the HST coordinates of $1''.26$. Since we know that we can not do better than the HST astrometry we follow the same method of registering the images by shifting the peak of the UV bright core to the center of the radio nucleus. This involves a shift

Table 1. MERLIN 20 cm parameters of the compact components in NGC 7319

Component	Position (J2000)		Flux density (mJy)	Size (arcsec)
	α	δ		
Compact A	$22^h 36^m 03.604^s$	$33^\circ 58' 33''.92$	7.86 ± 0.35 (mJy)	0.64×0.23
Compact B	$22^h 36^m 03.578^s$	$33^\circ 58' 33''.02$	1.07 ± 0.16 (mJy)	0.23×0.16
Compact C	$22^h 36^m 03.458^s$	$33^\circ 58' 30''.00$	3.68 ± 0.42 (mJy)	0.51×0.39

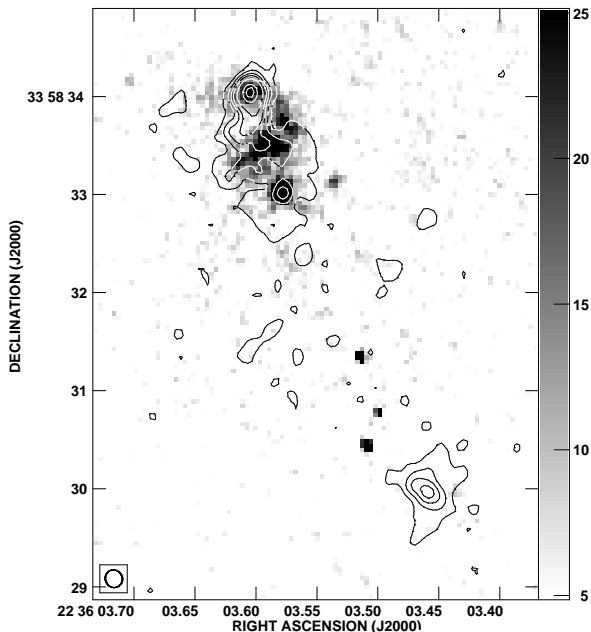


Figure 8. The 20 cm naturally weighted MERLIN image of NGC 7319 (resolution $0''.15$) overlaid on the ACS/HRC UV image. North is up and East to the left. The sidebar shows the relative intensity of the greyscale image. The contour levels have been set to $7.59e-5 \times (1, 2, 3, 4, 6, 8, 10, 12)$. The peak flux is 1.84 mJy/beam and the rms noise level is $\sim 47 \mu\text{Jy}/\text{beam}$. See text for discussion of aligned features.

of $0''.65$ in DEC (the shift in RA is subpixel, 6 mas). This shift is smaller than the HST astrometric uncertainties. Using this registration, contours of the MERLIN L-band image are overlaid on the HST/ACS image in Fig. 8.

Star formation is evident only in the bright core and the north lobe. There are only hints of UV emission from component C and three very compact regions of star formation, north of component C, trailing the region of the south lobe. The Ultraviolet emission starts from component B, the core, and has an extent that matches the north lobe (Fig. 9). The emission raps around the north lobe and strong star formation appears at the position of component A, the end hotspot of the north lobe. Almost midway between components A and B, an extended intense star formation region is almost perpendicular to the radio axis. The UV emission follows closely the elongated contours (jet-like extension) seen in the

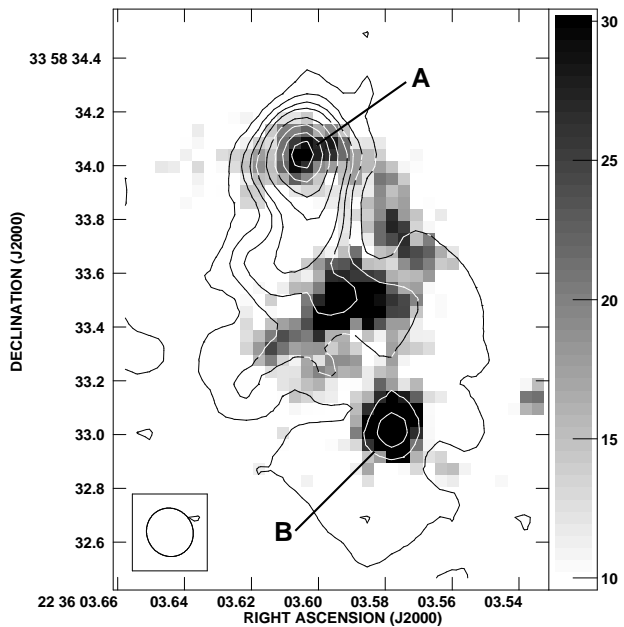


Figure 9. Enlarged image of Fig. 8 isolating the bright core and north lobe. See text for detailed description.

MERLIN image below component A. The SE-NW extent of this UV structure is $0''.85$ or 0.45 kpc. A $0''.13$ smoothed version of the HST/ACS UV image (Fig. 10) brings out an additional star formation region to the W of this region and just below to what seems now a more marked, pronounced and extended UV structure between components A and B, almost arclike in shape. A difference image (the smoothed image was subtracted from the original unsmoothed image) identifies the UV emission in the region of the core as the brightest UV region with the most intense star formation.

4 DISCUSSION

Based on the similar properties (strongly interacting galaxies with tidal tails and bridges, most spirals and S0s, X-ray emitting intragroup gas with similar X-ray properties) and the HI mass, Smith et al. (2003) have put forward an evolutionary scenario from spiral dominated groups to elliptical dominated groups. In this scheme Stephan's Quintet is probably in an intermediate transition state between HCG

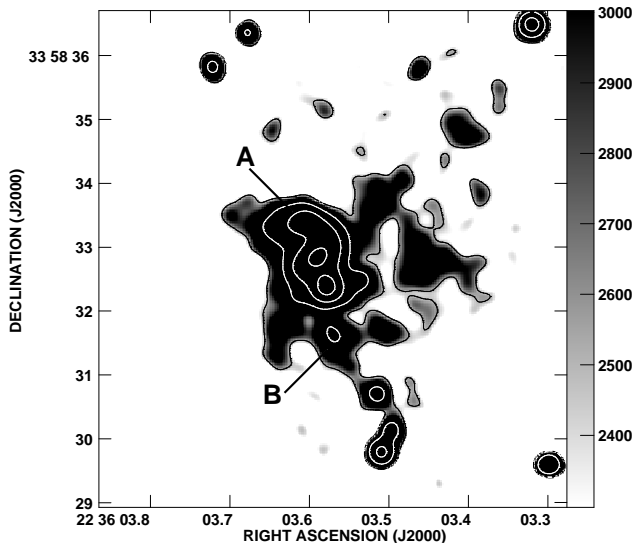


Figure 10. HST ACS/HRC UV image smoothed to $0''.13$ resolution. This enhances and reveals star formation to the West of NGC 7319.

16 (earlier stage), in which the HI mass is in both the inner region and tidal features, and NGC 4410 (later stage), with less HI mass than Stephan’s Quintet distributed mostly in the tidal features. The HI mass of Stephan’s Quintet ($M_{HI} \sim 10^{10} M_{\odot}$, Verdes-Montenegro et al. 2001) is mostly found outside the galaxies of the group and in tidal features. The galaxies have almost been completely stripped of their neutral hydrogen (Shostak et al. 1984, Williams et al. 2002). Interactions between the galaxies rather than ram pressure have been suggested by Verdes-Montenegro et al. (2001) to create HI rich tidal features while depleting the inner regions of galaxies of HI. NGC 4410 is also the only group of the three that contains a radio galaxy with radio lobes extending beyond the optical galaxy. The existence of large radio lobes in the merging galaxy NGC 4410A shows that such structures can occur fairly early in the formation of an elliptical, when it is not yet an elliptical (Smith et al. 2003). Both HCG 16 and Stephan’s Quintet contain Seyfert galaxies. However, in Stephan’s Quintet, a triple radio structure is also present within the dominant galaxy NGC 7319. Is NGC 7319 an example of a spiral galaxy in which jets are present but smothered by dense interstellar clouds as suggested by Wang et al. (2000)? The evidence in this paper seems to point to this. The jet-cloud interaction is evident in the arclike-structure seen in NGC 7319 midway between components B and A. We believe that incidence of the jet on the cloud/dense ambient gas at this region causes a strong bow-shock that is driven into the cloud and creates the bright star-formation perpendicular to the direction of the shock and aligned with the extended radio contours (see below for UV-radio correlation). The arclike shape of this structure, as revealed in the smoothed image, is further support of the presence of bow-shock (e.g. Bicknell et al. 2000). The jet deposits much of its momentum at this site and it continues upward to component A where the decelerated jet plasma

accumulates as a radio “lobe”. Wang et al. (2000) present a model in which weak and intermediate power jets can effectively be halted or destroyed by reasonably massive clouds and this can be related to the paucity of extended radio jets in spiral galaxies. After the jet impacts the cloud, it makes slow headway and finally is effectively stalled by the cloud. A tilted interaction area forms in front of the jet nonetheless the vortical backflow exerts pressure on the jet from the top side, thus causing the penetrating part of the jet to bent slightly downward. The curved structure seen at the very end of the UV continuum can be a result of the bent of the jet as the UV emission trails the radio emission. Eventually a very extensive cocoon forms on the top side of the jet and interaction between the cocoon and the jet induces the jet to evince a substantially wiggly structure.

But is there evidence of such a cloud and dense material in or near NGC 7319? Observational evidence for dense and cool gas in high redshift galaxies has been plentiful and includes the detection of dust, HI, extended line emission, associated absorption line systems and molecular gas (e.g. De Breuck et al. 2003). NGC 7319 has lost all detectable (upper limit $\sim 10^8 M_{\odot}$) HI, the vast majority of HII regions (expected in a typical \sim SBb spiral) and an uncertain fraction of stellar mass. At this epoch NGC 7319 is without an ISM that could sustain the star formation necessary to propagate and define a Population I spiral pattern. However, a very bright condensation of young blue stars is found in the northeast edge of the disk and both this $H\alpha$ and CO emission (Yun et al. 1997) in NGC 7319 is ~ 8 kpc north-northeast of the nucleus ($6.2 \times 10^8 M_{\odot}$). This region of material is most probably responsible for confining the North lobe within the spiral structure of NGC 7319. A second massive CO complex is found within 2 kpc of the nucleus (Yun et al. 1997), although Gao & Xu (2000) place this source on the nucleus. This material coincides with the UV bright core and is most possibly responsible for the birth of the bow-shock above the core. The inferred H_2 mass for NGC 7319 is $4-7 \times 10^9 M_{\odot}$ (Yun et al. 1997, Gao & Xu 2000, Smith & Struck 2001). The central region of NGC 7319 is luminous from X-ray to radio wavelengths. It contributes more than half of the MIR/FIR emission observed from SQ. ISOCAM observations of Stephan’s Quintet (Xu et al. 1999) in the $15 \mu m$ emission, a good nearly extinction-free star formation rate (SFR) indicator, show the strongest peak surface brightness on the Seyfert 2 nucleus of NGC 7319 with a flux of 79.8 mJy.

Alignment of the rest-frame UV continuum emission from the parent galaxies with the nonthermal radio emission has been discovered in high-redshift radio galaxies (McCarthy et al. 1987, Chambers et al. 1987). The nature of this continuum and “alignment effect” has remained however unclear. It appears that interactions between the radio plasma and the ambient gas determine the morphology of the UV with the radio ejecta sweeping up and compressing the interstellar medium. In nearby radio galaxies, evidence has been found for jet-induced star formation, scattered light from hidden quasar-like AGN and nebular recombination continuum (van Breugel 1985a,b, van Breugel & Dey 1993, Dey et al. 1996, Tadhunter et al. 1996, Cimatti et al. 1996). van Breugel et al. (2004) show that shocks associated with jets may trigger the collapse of clouds to form stars. Whether this occurs at the impact area, or along the sides of expand-

ing lobes depends on jet power and the ambient gas density distribution. It is natural to interpret enhanced UV continuum as tracing the locus of newly formed stars. NGC 7319 can most possibly be the first example of jet induced star formation in a Seyfert galaxy. Up to now there was little evidence for star formation in the nuclear region of NGC 7319 (e.g. Malkan et al. 1998, Yun et al. 1999). A bright UV core is seen for the first time in Fig. 7. The size of this compact emission is $0''.4$ or 195 pc. The star formation appears more pronounced to the N slightly displaced from the nucleus. Both the orientation and the elongation of this region is in perfect agreement with the blue elongated region $1''.1$ (533 pc) N of the nucleus at a PA of 10° , discovered by Kotilainen (1998) in a B–I map of NGC 7319. The UV and blue emission also agree well with the radio axis as well as with the [O III] and the blueward sloping asymmetry detected in the [O III] line profiles at the nucleus and northeast of the nucleus (Aoki et al. 1999). Kotilainen (1998) suggested the blue elongation might represent scattered light from the nucleus. However, he hinted at the idea that the blue structures that he saw in Seyfert 2 galaxies might be due to an intrinsically nonstellar continuum, e.g. emission from high velocity shock waves generated from the interaction of a radio jet with the extended Narrow Line Region Gas (e.g. Sutherland 1993). Such an explanation would require a very close morphological correlation between the continuum and the high velocity ionized gas which he was not finding. An accurate knot-to-knot and feature-to-feature matching between the UV structure and linear radio structure is however established in Fig. 8. Furthermore we have direct evidence for sharp boundaries and knotty UV morphology which is the signature of star forming regions. The extent of the UV emission is the same as the extent of the radio structure $\sim 5''$ (2.42 kpc) and at the same PA $\sim 25^\circ$, further supporting close correlation between jet emission and star formation. In addition, the UV emission in our Fig. 7 resembles the optical fine structure, similar to a curved jet, revealed in the difference WFPC2 (Fig. 5) of Aoki et al (1999)

The absence of any evidence for a polarized, scattered AGN continuum would support the notion that the active nucleus is not responsible for the extended UV emission. However, the hard X-ray emission, peaked on NGC 7319, is consistent with an absorbed powerlaw, and exhibits a strong Fe K line, providing strong evidence for an obscured nucleus in NGC 7319 (Awaki et al. 1997). Optical data (Aoki et al. 1996) also show a strong anisotropic nuclear ionization radiation which could be produced by an obscuring torus. On the other hand, the mass of molecular gas in the central complex observed, is $< 2 \times 10^8 M_\odot$, but this is inconsistent with the bulk of the observed MIR/FIR emission originating in a hidden nuclear burst (Xu et al. 1999). Furthermore, the data show that there is substantial turbulence produced by a jet-cloud interaction in the vicinity of the radio components B and A and that the emission lines from the galaxy are probably related either to the star-forming region or to emission from radiative cloud shocks rather than excitation by UV–X-ray emission from the active nucleus. The smoothed image shows further disturbed UV continuum associated with the extended structure between components B and A and this disturbance might have promoted more star formation unveiled in the smoothed image.

In summary, our high resolution radio observations of

Stephan's Quintet have shown that the Seyfert 2 galaxy, NGC 7319, has a flat spectrum core and two very asymmetrically distributed lobes with hotspots on opposite sides of the core. This adds to the evidence which calls into question the usual assumption that the compact radio components of Seyfert galaxies represent the galaxy nucleus. A knot-to-knot morphological correlation between this triple radio structure and UV emission unveiled in an HST/ACS HRC image of NGC 7319 may suggest that star formation in this Seyfert galaxy is induced by the collision of a jet with dense ambient material. We plan to present a detail analysis (star formation rates and kinematical data) for the UV components in NGC 7319, as well as a proposed model/simulation for the jet-cloud interaction in a follow-up paper. We then hope to also answer the question of whether NGC 7319 will eventually evolve into a classical double-lobed radio galaxy. To our knowledge, this may well be the first example of jet induced star-formation in a Seyfert galaxy.

ACKNOWLEDGMENTS

MERLIN is operated as a National Facility by the Jodrell Bank Observatory, University of Manchester, on behalf of the UK Particle Physics & Astronomy Research Council. The VLA is operated by the National Radio Astronomy Observatory which is supported by the National Science Foundation operated under cooperative agreement by Associated Universities, Inc. This research was supported by European Commission, TMR Programme, Research Network Contract ERBFMRXCT96-0034 "CERES". EXs work was performed under the auspices of the U.S. Department of Energy, National Nuclear Security Administration by the University of California, Lawrence Livermore National Laboratory under contract No. W-7405-Eng-48 and she also acknowledges support from the National Science Foundation (grant AST 00-98355). The authors would like to thank the anonymous referee for helpful suggestions that improved the presentation of this work.

REFERENCES

- Allen, R. J., Hartsuiker, J. W., 1972, *Nature*, 239, 324
- Allen, R. J., Sullivan, W., 1980, *A&A*, 84, 181
- Aoki, K., Ohtani, H., Yoshida, M., Kosugi, G., 1996, *AJ*, 111, 140
- Aoki, K., Kosugi, G., Wilson, A. S., Yoshida, M., 1999, *ApJ*, 521, 565
- Awaki, H., Koyama, K., Matsumoto, H., et al., 1997, *PASJ*, 49, 445
- Baars, J. W. M., Genzel, R., Pauliny-Toth, I. I. K., Witzel, A., 1977, *A&A*, 61, 99
- Bicknell, G. V., Sutherland, R. S., van Breugel, W. J. M., Dopita, M. A., Dey, A., Miley, G. K., 2000, *ApJ*, 540, 678
- Bushouse, H. A., 1987, *ApJ*, 320, 49
- Chambers, K. C., Miley, G. K., van Breugel, W., 1987, *Nature*, 329, 604
- Cimatti, A., Dey, A., van Breugel, W. J. M., Antonucci, R., Spinrad, H., 1996, *ApJ*, 465, 145
- Clements, F. D., 1983, *MNRAS*, 204, 811
- De Breuk, C., et al., 2003, *A&A*, 401, 911
- Dey, A., Cimatti, A., van Breugel, W. J. M., Antonucci, R., Spinrad, H., 1996, *ApJ*, 465, 157
- Durret, F., 1987, *A&ASS*, 105, 57

- Gao, Yu, Xu, C., 2000, *ApJ*, 542, L83
Hickson, P., 1982, *ApJ*, 475, L21
Kotilainen, J. K., 1998, *A&AS*, 132, 197
Kukula, M. J., Ghosh, T., Pedlar, A., Schilizzi, R. T., 1999, *ApJ*, 518, 117
McCarthy, P. J., van Breugel, W. Spinrad, H., Djorgovski, S., 1987, *ApJ*, 321, L29
Malkan, M., Gorjian, V., Tam, R. 1998, *ApJS*, 117, 25
Mendes de Oliveira, C., Plana, H., Amram, P., Balkowski, C., Bolte, M., 2001, *AJ*, 121, 2524
Menon, T. K., 1995, *MNRAS*, 274, 845
Mobasher, B., Cram, L., Georgakakis, A., Hopkins, A., 1999, *MNRAS*, 308, 45
Moles, M., Sulentic, J. W., Márquez, I., 1997, *ApJ*, 485, L69
Moles, M., Márquez, I., Sulentic, J. W., 1998, *A&A*, 334, 473
Morganti, R., Oosterloo, T., Tsvetanov, Z., 1998, *AJ*, 115, 915
Pietsch, W., Trinchieri, G., Arp, H., and Sulentic, J. W., 1997, *A&A*, 322, 89
Shostak, G. S., Sullivan III, W. T., Allen, R. J., 1984, *A&A*, 139, 15
Smith, B., Struck, C., 2001, *AJ*, 121, 710
Smith, B., Nowak, M., Donahue, M., Stocke, J., 2003, *AJ*, 126, 1763
Stephan, M. E., 1877, *C. R. Acad. Sci. Paris*, 84, 641
Su, B. M., Muxlow, T. W. B., Pedlar, A., Holloway, A. J., Steffen, W., Kukula, M. J., Mutel, R. L., 1996, *MNRAS*, 279, 1111
Sulentic, J. W., Arp, H., 1983, *AJ*, 88, 267
Sulentic, J. W., Rosaldo, M., Dultzin-Hacyan, D., Verdes-Montenegro, L., Trinchieri, G., Xu, G., Pietsch, W., 2001, *AJ*, 122, 2993
Sutherland, R. S., Bicknell, G. V., Dopita, M. A., 1993, *ApJ*, 414, 510
Tadhunter, C. N., Dickson, R. C., Shaw, M. A., 1996, *MNRAS*, 281, 591
Thean, A., Pedlar, A., Kukula, M. J., Baum, S. A., O'Dea, C. P., 2000, *MNRAS*, 314, 573
Thean, A., Pedlar, A., Kukula, M. J., Baum, S. A., O'Dea, C. P., 2001, *MNRAS*, 325, 737
van Breugel, W. J. M., Filipenko, A. V., Heckman, T., Miley, G. K., 1985a, *ApJ*, 293, 83
van Breugel, W. J. M., Miley, G. K., Heckman, T., Butcher, H., Bridle, A., 1985b, *ApJ*, 290, 496
van Breugel, W. J. M., Dey, A., 1993, *ApJ*, 414, 563
van Breugel, W., Fragile, C., Anninos, P., Murray, S., 2004, in *Recycling Intergalactic and Interstellar Matter*, IAU Symposium Series, eds. Pierre-Alain, Duc, Jonathan Braine, Elias Brinks, Vol. 217, E29
van der Hulst, J. M., Rots, A. H., 1981, *AJ*, 86, 1775
Verdes-Montenegro, L., Yun, M. S., Williams, B. A., Huchtmeier, W. K., Del Olmo, A., Perea, J., *A&A*, 377, 812
Wang, Z., Wiita, P. J., Hooda, J. S., 2000, *ApJ*, 534, 201
Williams, B. A., 1998, *AAS* 192, # 25.05
Williams, B. A., Yun, M. S., Verdes-Montenegro, L., 2002, *AJ*, 123, 2417
Xu, C., Sulentic, J. W., Tuffs, R., 1999, *ApJ*, 512, 178
Xu, C., Lu, N., Condon, J. J., Dopita, M., Tuffs, R. J., 2003, *ApJ*, 595, 665
Yun, M. S., Verdes-Montenegro, L., Del Olmo, A., Perea, J., 1997, *ApJ*, 475, L21